

Electromagnetic transitions among octet and decuplet baryons in QCD

T. M. Aliev ^{*†}, Y. Öktem [‡], M. Savcı [§]

Physics Department, Middle East Technical University, 06531 Ankara, Turkey

[‡] Physics Department, Faculty of Sciences, İstanbul University,
Vezneciler, 34134 İstanbul, Turkey

Abstract

The magnetic dipole $G_M(Q^2)$, electric quadrupole $G_E(Q^2)$, and Coulomb quadrupole $G_C(Q^2)$ form factors, describing the spin-3/2 to spin-1/2 electromagnetic transitions, are investigated within the light cone QCD sum rules. The Q^2 dependence of these form factors, as well as ratios of electric quadrupole and Coulomb quadrupole form factors to the magnetic dipole form factors are studied. We also compare our results on the magnetic dipole form factor with the prediction of the covariant spectator quark model.

PACS numbers: 11.55.Hx, 13.30.Ce, 13.40.Gp, 14.20.Jn

*e-mail: taliev@metu.edu.tr

†permanent address: Institute of Physics, Baku, Azerbaijan

‡e-mail: sgyks@istanbul.edu.tr

§e-mail: savci@metu.edu.tr

1 Introduction

According to the SU(3) classification of the baryons, spin-1/2 and spin-3/2 baryons belong to the octet and decuplet representations, respectively. The electromagnetic properties of octet and decuplet baryons, as well as octet to decuplet transitions are characterized by their electromagnetic form factors. As is well known, form factors carry essential information about the internal structure of baryons, i.e., about their charge and current distribution. The octet to decuplet electromagnetic transition is described with the help of the magnetic dipole (M1), electric quadrupole (E2) and Coulomb quadrupole (C2) form factors, which follow from the spin-parity selection rule.

At present, rich experimental data have been accumulated on electromagnetic and $\gamma^*N \rightarrow \Delta$ transition form factors (see [1] and references therein), while the data for other possible γ^* octet \rightarrow decuplet transitions are practically absent (very limited data can be found in [2, 3]). The octet to decuplet electromagnetic transitions are studied within different theoretical approaches, such as the quark model [4–7], QCD sum rules [8, 9], and lattice QCD [10]. In many theoretical works, the octet to decuplet electromagnetic transitions have been studied at $Q^2 = 0$, but only in a few works have the form factors of these transitions been studied. These form factors were studied in the framework of the covariant quark model in [11] and in lattice QCD in [12], for the $\gamma^*N \rightarrow \Delta$ transition only, and were investigated in light cone QCD sum rules in [13], respectively.

In the present work we study the octet to decuplet transition form factors within the light cone QCD sum rules. Note that these form factors are calculated within the same approach at $Q^2 = 0$ in [9]. The plan of the work is as follows. In the following section we derive the sum rules for the form factors responsible for the octet to decuplet electromagnetic transition, whose numerical analysis is performed in Sec. 3. This section also contains a comparison of our results with other approaches and conclusions.

2 Sum rules for the octet to decuplet electromagnetic transition form factors

In the present section we derive sum rules for the octet to decuplet electromagnetic transition form factors. For this purpose we consider the following correlator function,

$$\Pi_{\mu\nu}(p, q) = i \int d^4x e^{iqx} \left\langle 0 \left| T \left\{ \eta_\mu(0) j_\nu^{el}(x) \right\} \right| \mathcal{O}(p) \right\rangle, \quad (1)$$

where η_μ is the interpolating current for the relevant decuplet baryon; $\mathcal{O}(p)$ represents an octet baryon with momentum p ; $j_\nu^{el} = e_u \bar{u} \gamma_\nu u + e_d \bar{d} \gamma_\nu d + e_s \bar{s} \gamma_\nu s$ is the electromagnetic current; q is its four-momentum; and e_u , e_d , and e_s are the charges of u , d and s quarks, respectively. The interpolating current of decuplet baryons can be written as,

$$\eta_\mu = N \varepsilon^{abc} \left\{ (q_1^{aT} C \gamma_\mu q_2^b) q_3^c + (q_2^{aT} C \gamma_\mu q_3^b) q_1^c + (q_3^{aT} C \gamma_\mu q_1^b) q_2^c \right\},$$

where a , b , and c are the color indices and C is the charge conjugation operator. The quark content q_1 , q_2 , and q_3 and the normalization factor N of each decuplet baryon are given in Table 1.

	N	q_1	q_2	q_3
Σ^{*+}	$\sqrt{1/3}$	u	u	s
Σ^{*0}	$\sqrt{2/3}$	u	d	s
Σ^{*-}	$\sqrt{1/3}$	d	d	s
Ξ^{*0}	$\sqrt{1/3}$	s	s	u
Ξ^{*-}	$\sqrt{1/3}$	s	s	d

Table 1: Quark content and the value of normalization factor N in interpolating current of the decuplet baryons

The form factors which describe the octet to decuplet electromagnetic transition are defined by the matrix element of the j_ν^{el} sandwiched between the members of the decuplet and octet baryon states with momenta p' and p , respectively. By virtue of Lorentz invariance and current conservation, this matrix element can be written in terms of three form factors as follows [14]:

$$\begin{aligned} \langle \mathcal{D}(p') | j_\nu^{el} | \mathcal{O}(p) \rangle = & \bar{u}_\alpha(p') \left\{ G_1(Q^2) \left(-q_\alpha \gamma_\nu + \not{q} g_{\alpha\nu} \right) + \frac{G_2(Q^2)}{2} \left[-q_\alpha \mathcal{P}_\nu + (q \cdot \mathcal{P}) g_{\alpha\nu} \right] \right. \\ & \left. + G_3(Q^2) \left[q_\alpha q_\nu - q^2 g_{\alpha\nu} \right] \right\} \gamma_5 u(p) , \end{aligned} \quad (2)$$

where $\mathcal{P} = \frac{1}{2}(p' + p) = \frac{1}{2}(2p - q)$, and $u_\alpha(p')$ is the spin-3/2 Rarita-Schwinger spinor. From an experimental point of view, the so-called multipole form factors are more suitable and we shall use this set of form factors in further analysis. The relations among the form factors G_1 , G_2 , G_3 and the multipole form factors, namely, magnetic dipole $G_M(Q^2)$, electric quadrupole $G_E(Q^2)$, and Coulomb quadrupole $G_C(Q^2)$ form factors, are given as [14]

$$\begin{aligned} G_M(Q^2) = & \frac{m_{\mathcal{D}}}{3(m_{\mathcal{D}} + m_{\mathcal{O}})} \left\{ \left[(3m_{\mathcal{D}} + m_{\mathcal{O}})(m_{\mathcal{D}} + m_{\mathcal{O}}) + Q^2 \right] \frac{G_1(Q^2)}{m_{\mathcal{D}}} \right. \\ & \left. + (m_{\mathcal{D}}^2 - m_{\mathcal{O}}^2)G_2(Q^2) - 2Q^2G_3(Q^2) \right\} , \\ G_E(Q^2) = & \frac{m_{\mathcal{D}}}{3(m_{\mathcal{D}} + m_{\mathcal{O}})} \left\{ (m_{\mathcal{D}}^2 - m_{\mathcal{O}}^2 - Q^2) \frac{G_1(Q^2)}{m_{\mathcal{D}}} + (m_{\mathcal{D}}^2 - m_{\mathcal{O}}^2)G_2(Q^2) - 2Q^2G_3(Q^2) \right\} , \\ G_C(Q^2) = & \frac{2m_{\mathcal{D}}}{3(m_{\mathcal{D}} + m_{\mathcal{O}})} \left\{ 2m_{\mathcal{D}}G_1(Q^2) + (3m_{\mathcal{D}}^2 + m_{\mathcal{O}}^2 + Q^2) \frac{G_2(Q^2)}{2} \right. \\ & \left. + (m_{\mathcal{D}}^2 - m_{\mathcal{O}}^2 - Q^2)G_3(Q^2) \right\} . \end{aligned} \quad (3)$$

In further analysis we shall also study the dependence of the ratios of the electric $G_E(Q^2)$ and Coulomb $G_C(Q^2)$ quadrupole form factors to the dipole form factor $G_M(Q^2)$. Note that

these ratios are measured in experiments for the $\gamma^* N \rightarrow \Delta$ transitions which are defined as

$$\begin{aligned} R_{EM}(Q^2) &= -\frac{G_E(Q^2)}{G_M(Q^2)}, \\ R_{SM}(Q^2) &= -\frac{G_C(Q^2)}{2m_{\mathcal{D}}G_M(Q^2)} \sqrt{Q^2 + \frac{(m_{\mathcal{D}}^2 - m_{\mathcal{O}}^2 - Q^2)^2}{m_{\mathcal{D}}^2}}. \end{aligned} \quad (4)$$

In order to derive the sum rules for the octet to decuplet transition form factors we calculate the correlator function in terms of hadronic and quark–gluon degrees of freedom.

The contribution of the decuplet baryons to the correlation function (1) is obtained in the following way,

$$\Pi_{\mu\nu} = \frac{1}{m_{\mathcal{D}}^2 - p'^2} \langle 0 | \eta_{\mu}(0) | \mathcal{D}(p') \rangle \langle \mathcal{D}(p') | j_{\nu}^{el}(x) | \mathcal{O}(p) \rangle + \dots, \quad (5)$$

where \dots refers to the contributions of the higher states with the same quantum numbers as decuplet baryons. The matrix element $\langle 0 | \eta_{\mu}(0) | \mathcal{D}(p') \rangle$ is determined as

$$\langle 0 | \eta_{\mu}(0) | \mathcal{D}(p') \rangle = \lambda_{\mathcal{D}} u_{\mu}(p'), \quad (6)$$

where $\lambda_{\mathcal{D}}$ is the residue for the corresponding decuplet baryon. The matrix element $\langle \mathcal{D}(p') | j_{\nu}^{el}(x) | \mathcal{O}(p) \rangle$ can be expressed in terms of three form factors G_1 , G_2 and G_3 with the help of Eq. (2). Summation over spins of spin-3/2 baryons is defined as,

$$\sum_s u_{\mu}(p', s) \bar{u}_{\alpha}(p', s) = -(p' + m_{\mathcal{D}}) \left[g_{\mu\alpha} - \frac{1}{3} \gamma_{\mu} \gamma_{\alpha} - \frac{2p'_{\mu} p'_{\alpha}}{3m_{\mathcal{D}}^2} + \frac{p'_{\mu} \gamma_{\alpha} - p'_{\alpha} \gamma_{\mu}}{3m_{\mathcal{D}}} \right]. \quad (7)$$

The contributions of the decuplet baryons to the correlation function can be obtained by substituting Eqs. (2) and (3) in Eq. (5), from which we get

$$\begin{aligned} \Pi_{\mu\nu}(p, q) &= -\frac{1}{m_{\mathcal{D}}^2 - p'^2} \lambda_{\mathcal{D}} (p' + m_{\mathcal{D}}) \left[g_{\mu\alpha} - \frac{1}{3} \gamma_{\mu} \gamma_{\alpha} - \frac{2p'_{\mu} p'_{\alpha}}{3m_{\mathcal{D}}^2} + \frac{p'_{\mu} \gamma_{\alpha} - p'_{\alpha} \gamma_{\mu}}{3m_{\mathcal{D}}} \right] \\ &\times \left\{ G_1(Q^2) (\bar{q}_{\alpha} \gamma_{\nu} + \not{q} g_{\alpha\nu}) + \frac{G_2(Q^2)}{2} [-q_{\alpha} \mathcal{P}_{\nu} + (q \cdot \mathcal{P}) g_{\alpha\nu}] \right. \\ &\left. + G_3(Q^2) [q_{\alpha} q_{\nu} - q^2 g_{\alpha\nu}] \right\} \gamma_5 u(p). \end{aligned} \quad (8)$$

It should be remarked here that Eq. (4) contains contributions not only from the decuplet baryons, but also from spin–parity $1^-/2$ baryons. Indeed, the matrix elements of the η_{μ} current sandwiched between vacuum and the spin–parity $1^-/2$ state (denoted by \mathcal{D}^*) is determined as

$$\langle 0 | \eta_{\mu}(0) | \mathcal{D}^*(p') \rangle = A(\gamma_{\mu} m_* - 4p'_{\mu}) u^*(p'). \quad (9)$$

It follows from Eq. (5) that the unwanted spin-1/2 contribution contains terms multiplied by p' or γ_{μ} at left, which all must be eliminated. For this purpose an ordering procedure of Dirac matrices is needed, as the result of which we also obtain the independent structures.

In this work we choose the ordering of the Dirac matrices as $\gamma_\mu \not{p}' \not{q} \gamma_\nu \gamma_5$. After eliminating the contributions of the spin-1/2 baryons, the correlation function takes the following form:

$$\begin{aligned} \Pi_{\mu\nu}(p, q) = & -\frac{1}{m_{\mathcal{D}}^2 - p'^2} \lambda_{\mathcal{D}} (\not{p}' + m_{\mathcal{D}}) \left\{ (-q_\mu \gamma_\nu + \not{q} g_{\mu\nu}) G_1(Q^2) \right. \\ & \left. + \left[-q_\mu \mathcal{P}_\nu + (q \cdot \mathcal{P}) g_{\mu\nu} \right] \frac{G_2(Q^2)}{2} + \left[q_\mu q_\nu - q^2 g_{\mu\nu} \right] G_3(Q^2) \right\} \gamma_5 u(p) . \quad (10) \end{aligned}$$

The above expression for the correlation function can be decomposed into contributions of various Lorentz structures, any three of which can be used in the numerical calculations of the form factors G_1 , G_2 and G_3 . In the present work we choose the structures $\not{p}' \not{q} \gamma_5 g_{\mu\nu}$, $\not{p}' \gamma_5 q_\mu p'_\nu$ and $\not{p}' \gamma_5 q_\mu q_\nu$, in determination of the form factors G_1 , G_2 and $\frac{G_2}{2} - G_3$, respectively. The invariant functions in the correlation function corresponding to the structures $\not{p}' \not{q} \gamma_5 g_{\mu\nu}$, $\not{p}' \gamma_5 q_\mu p'_\nu$ and $\not{p}' \gamma_5 q_\mu q_\nu$ are given as,

$$\begin{aligned} \Pi^{(1)} &= -\frac{\lambda_{\mathcal{D}}}{m_{\mathcal{D}}^2 - p'^2} G_1(Q^2) , \\ \Pi^{(2)} &= \frac{\lambda_{\mathcal{D}}}{m_{\mathcal{D}}^2 - p'^2} G_2(Q^2) , \\ \Pi^{(3)} &= \frac{\lambda_{\mathcal{D}}}{m_{\mathcal{D}}^2 - p'^2} \left[\frac{G_2(Q^2)}{2} - G_3(Q^2) \right] , \quad (11) \end{aligned}$$

respectively. In order to construct sum rules for the form factors G_1 , G_2 and $\frac{G_2}{2} - G_3$ we need the corresponding expressions of the correlation function from the QCD side, in which distribution amplitudes (DAs) of the octet baryons are contained. Since the $\gamma^* N \rightarrow \Delta$ transition has already been investigated in the framework of the QCD sum rules in [13], we restrict our analysis to the consideration of the $\gamma^* \Sigma \rightarrow \Sigma^*$, $\gamma^* \Lambda \rightarrow \Sigma^*$, and $\gamma^* \Xi \rightarrow \Xi^*$ transitions.

The distribution amplitudes of the octet baryons are defined as a matrix element of the three-quark operator between one of the members of the octet baryon and vacuum, i.e.,

$$\varepsilon^{abc} \langle 0 | q_{1\alpha}^a(a_1 x) q_{2\beta}^b(a_2 x) q_{3\gamma}^c(a_3 x) | \mathcal{O}(p) \rangle ,$$

where a, b, c are the color indices; α, β and γ are the Lorentz indices; and a_i are positive numbers satisfying $a_1 + a_2 + a_3 = 1$.

Lorentz covariance, together with spin and parity of the baryons, imposes that the general Lorentz composition of the matrix element is

$$4\varepsilon^{abc} \langle 0 | q_{1\alpha}^a(a_1 x) q_{2\beta}^b(a_2 x) q_{3\gamma}^c(a_3 x) | \mathcal{O}(p) \rangle = \sum_i \mathcal{F}_i \Gamma_{\alpha\beta}^{1i} \left(\Gamma^{2i} \mathcal{O}(p) \right)_\gamma , \quad (12)$$

where $\Gamma^{1(2)i}$ are certain Dirac matrices, and $\mathcal{F}_i = \mathcal{S}_i, \mathcal{P}_i, \mathcal{A}_i, \mathcal{V}_i$ and \mathcal{T}_i are the DAs having no definite twists. This decomposition in terms of the functions \mathcal{F}_i can be found in [15], and for completeness it is presented in Appendix A.

The DAs with definite twist are given as,

$$4\varepsilon^{abc}\langle 0 | q_{1\alpha}^a(a_1x)q_{2\beta}^b(a_2x)q_{3\gamma}^c(a_3x) | \mathcal{O}(p) \rangle = \sum_i F_i \Gamma_{\alpha\beta}^{1i} \left(\Gamma^{2i} \mathcal{O}(p) \right)_\gamma, \quad (13)$$

where $F_i = S_i, P_i, A_i, V_i, A_i$ and T_i . The relations among these two sets of DAs are given as,

$$\begin{aligned} \mathcal{S}_1 &= S_1, & (2P \cdot x) \mathcal{S}_2 &= S_1 - S_2, \\ \mathcal{P}_1 &= P_1, & (2P \cdot x) \mathcal{P}_2 &= P_2 - P_1, \\ \mathcal{V}_1 &= V_1, & (2P \cdot x) \mathcal{V}_2 &= V_1 - V_2 - V_3, \\ 2\mathcal{V}_3 &= V_3, & (4P \cdot x) \mathcal{V}_4 &= -2V_1 + V_3 + V_4 + 2V_5, \\ (4P \cdot x) \mathcal{V}_5 &= V_4 - V_3, & (2P \cdot x)^2 \mathcal{V}_6 &= -V_1 + V_2 + V_3 + V_4 + V_5 - V_6, \\ \mathcal{A}_1 &= A_1, & (2P \cdot x) \mathcal{A}_2 &= -A_1 + A_2 - A_3, \\ 2\mathcal{A}_3 &= A_3, & (4P \cdot x) \mathcal{A}_4 &= -2A_1 - A_3 - A_4 + 2A_5, \\ (4P \cdot x) \mathcal{A}_5 &= A_3 - A_4, & (2P \cdot x)^2 \mathcal{A}_6 &= A_1 - A_2 + A_3 + A_4 - A_5 + A_6, \\ \mathcal{T}_1 &= T_1, & (2P \cdot x) \mathcal{T}_2 &= T_1 + T_2 - 2T_3, \\ 2\mathcal{T}_3 &= T_7, & (2P \cdot x) \mathcal{T}_4 &= T_1 - T_2 - 2T_7, \\ (2P \cdot x) \mathcal{T}_5 &= -T_1 + T_5 + 2T_8, & (2P \cdot x)^2 \mathcal{T}_6 &= 2T_2 - 2T_3 - 2T_4 + 2T_5 + 2T_7 + 2T_8, \\ (4P \cdot x) \mathcal{T}_7 &= T_7 - T_8, & (2P \cdot x)^2 \mathcal{T}_8 &= -T_1 + T_2 + T_5 - T_6 + 2T_7 + 2T_8. \end{aligned}$$

Explicit expressions of DAs $\mathcal{S}_i, \mathcal{P}_i, \mathcal{A}_i, \mathcal{V}_i$ and \mathcal{T}_i at the leading order of conformal spin expansion can be found in [8–11].

After lengthy calculations, we obtain the invariant functions Π_i for the γ^* *octet* \rightarrow *decuplet* transitions. Schematically, the expressions for Π_i can be written in terms of the functions $\rho_2(x), \rho_4(x)$, and $\rho_6(x)$ as follows:

$$\Pi = N \int_0^1 dx \left\{ \frac{\rho_2(x)}{(q - px)^2} + \frac{\rho_4(x)}{(q - px)^4} + \frac{\rho_6(x)}{(q - px)^6} \right\}. \quad (14)$$

Explicit expressions of the functions $\rho_2(x), \rho_4(x)$, and $\rho_6(x)$ for the considered transitions are given in Appendix B.

Equating the invariant functions $\Pi_i(Q^2)$, ($i = 1, 2, 3$) from the QCD and hadronic sides, and performing Borel transformation over the variable $-(p - q)^2$, we obtain the following sum rules for the form factors $G_i(Q^2)$:

$$\begin{aligned} G_i^\alpha(Q^2) &= \frac{N_\alpha}{2\lambda_{\mathcal{D}}} e^{m_{\mathcal{D}}^2/M^2} \left\{ \int_{x_0}^1 dx \left(-\frac{(\rho_2(x))_i^\alpha}{x} + \frac{(\rho_4(x))_i^\alpha}{x^2 M^2} - \frac{(\rho_6(x))_i^\alpha}{2x^3 M^4} \right) e^{-\frac{\bar{x}Q^2}{xM^2} - \frac{\bar{x}m_{\mathcal{O}}^2}{M^2}} \right. \\ &+ \left[\frac{(\rho_4(x_0))_i^\alpha}{Q^2 + x_0^2 m_{\mathcal{O}}^2} - \frac{1}{2x_0} \frac{(\rho_6(x_0))_i^\alpha}{(Q^2 + x_0^2 m_{\mathcal{O}}^2)M^2} \right. \\ &\left. \left. + \frac{1}{2} \frac{x_0^2}{(Q^2 + x_0^2 m_{\mathcal{O}}^2)} \left(\frac{d}{dx_0} \frac{(\rho_6(x_0))_i^\alpha}{x_0(Q^2 + x_0^2 m_{\mathcal{O}}^2)M^2} \right) \right] e^{-s_0/M^2} \right\}, \quad (15) \end{aligned}$$

where $i = 1, 2, 3$ correspond to the form factors $G_1(Q^2), G_2(Q^2), \frac{G_2(Q^2)}{2} - G_3(Q^2)$, and α corresponds to any member of the decuplet. Here M^2 is the square of the Borel mass

parameter, $s = \frac{\bar{x}}{x}Q^2 + \bar{x}m_{\mathcal{O}}^2$, x_0 is the solution of the equation $s = s_0$, $m_{\mathcal{O}}$ and $m_{\mathcal{D}}$ are masses of the members of the octet and decuplet baryons, respectively, and $\bar{x} = 1 - x$.

As has already been noted, the $\gamma^*N \rightarrow \Delta$ transition is studied within the light cone QCD sum rules in [13]; hence, we do not consider it in this work.

The sum rules needed in determining the three form factors $G_1(Q^2)$, $G_2(Q^2)$, and $\frac{G_2(Q^2)}{2} - G_3(Q^2)$ are given in Eq. (15). The form factors $G_1(Q^2)$ and $G_2(Q^2)$ are obtained from Eqs. (15). With the help of these three form factors, we finally rewrite our results in terms of the magnetic dipole $G_M(Q^2)$, electric quadrupole $G_E(Q^2)$, and Coulomb quadrupole $G_C(Q^2)$ form factors.

3 Numerical Analysis

In this section we present our numerical result for the magnetic dipole $G_M(Q^2)$, electric quadrupole $G_E(Q^2)$, and Coulomb quadrupole $G_C(Q^2)$ form factors. It follows from the explicit expressions of the sum rules for these form factors that in order to determine these form factors, DAs of the octet baryons are needed. A few words about the DAs of the octet baryons are in order. The distribution amplitudes of the nucleon within the next-to-leading order in conformal spin are calculated in [15]. These results are then extended to next-to-next order by calculating DAs with twist-3 in conformal spin in [16]. In the present work, we shall use DAs of the Λ , Σ , and Ξ octet baryons which are given in [17–20], and exclude these contributions, which have not yet been calculated.

The nonperturbative parameters $f_{\mathcal{O}}$, λ_1 , λ_2 and λ_3 appearing in the expressions of the DAs are given in [17–20], which are determined from the analysis of the two-point correlation function.

$$\begin{aligned} f_{\Xi} &= (9.9 \pm 0.4) \times 10^{-3} \text{ GeV}^2, \\ \lambda_1 &= -(2.1 \pm 0.1) \times 10^{-2} \text{ GeV}^2, \\ \lambda_2 &= (5.2 \pm 0.2) \times 10^{-2} \text{ GeV}^2, \\ \lambda_3 &= (1.7 \pm 0.1) \times 10^{-2} \text{ GeV}^2, \end{aligned}$$

$$\begin{aligned} f_{\Sigma} &= (9.4 \pm 0.4) \times 10^{-3} \text{ GeV}^2, \\ \lambda_1 &= -(2.5 \pm 0.1) \times 10^{-2} \text{ GeV}^2, \\ \lambda_2 &= (4.4 \pm 0.1) \times 10^{-2} \text{ GeV}^2, \\ \lambda_3 &= (2.0 \pm 0.1) \times 10^{-2} \text{ GeV}^2, \end{aligned}$$

$$\begin{aligned} f_{\Lambda} &= (6.0 \pm 0.3) \times 10^{-3} \text{ GeV}^2, \\ \lambda_1 &= (1.0 \pm 0.3) \times 10^{-2} \text{ GeV}^2, \\ |\lambda_2| &= (0.83 \pm 0.05) \times 10^{-2} \text{ GeV}^2, \\ |\lambda_3| &= (0.83 \pm 0.05) \times 10^{-2} \text{ GeV}^2. \end{aligned}$$

Furthermore, in calculating the form factors from the QCD sum rules analysis we need to find the working regions of the Borel mass parameter M^2 and continuum threshold s_0 . The continuum threshold is not completely arbitrary, and depends on the energy of the first excited states with the same quantum numbers. In our numerical calculations we will use $s_0 = 4.0 \text{ GeV}^2$ which is obtained from the mass sum rule analysis [21]. The working region of M^2 can be found by using the following criteria.

- The lower limit of M^2 is determined by demanding that the contributions coming from the higher states and continuum are less than half of the total result.
- The upper bound can be obtained by imposing the conditions required by the operator product expansion.

It follows from the numerical calculations that these two conditions are both fulfilled in the region $1.5 \leq M^2 \leq 3.5 \text{ GeV}^2$.

In the expressions of the form factors we see that the residues of the decuplet baryons are needed. These residues are calculated in [9], which we shall use in further numerical analysis.

We have already noted, from an experimental point of view, that the multipole form factors constitute a more suitable set compared to the form factors G_1 , G_2 and G_3 . For this reason, we will present the results for multipole form factors.

In Figs. (1)–(3), we present the Q^2 dependence of the magnetic dipole $G_M(Q^2)$, electric quadrupole $G_E(Q^2)$, and Coulomb quadrupole $G_C(Q^2)$ form factors for the $\gamma^*\Sigma^+ \rightarrow \Sigma^{*+}$ transition, at $s_0 = 4.0 \text{ GeV}^2$ and at several different values of the Borel mass parameter M^2 . In the numerical calculations Q^2 is varied in the region $1.0 \leq Q^2 \leq 8.0 \text{ GeV}^2$, because in this region the higher twist contributions and the higher states and continuum contributions are small.

It follows from these figures that the electric quadrupole form factor $G_E(Q^2)$ is small compared to the magnetic dipole form factor $G_M(Q^2)$.

Figures (4)–(8) depict the dependence of the magnetic dipole form factor $G_M(Q^2)$ on Q^2 , at $s_0 = 4.0 \text{ GeV}^2$ and at several different values of M^2 , for the $\gamma^*\Lambda \rightarrow \Sigma^{*0}$, $\gamma^*\Sigma^0 \rightarrow \Sigma^{*0}$, $\gamma^*\Sigma^- \rightarrow \Sigma^{*-}$, $\gamma^*\Xi^- \rightarrow \Xi^{*-}$, and $\gamma^*\Xi^0 \rightarrow \Xi^{*0}$, transitions, respectively. We see from these figures that the magnitude of the magnetic dipole form factors $G_M(Q^2)$ for the $\gamma^*\Xi^0 \rightarrow \Xi^{*0}$ and $\gamma^*\Sigma^+ \rightarrow \Sigma^{*+}$ transitions are practically equal. We also observe that the value of $G_M(Q^2)$ is quite small for the $\gamma^*\Sigma^- \rightarrow \Sigma^{*-}$ transition and is small for the $\gamma^*\Xi^- \rightarrow \Xi^{*-}$ transition. So, had the magnitudes of the magnetic dipole form factor $G_M(Q^2)$ been classified, they could be ordered as large for $\gamma^*\Sigma^+ \rightarrow \Sigma^{*+}$, moderate for $\gamma^*\Lambda \rightarrow \Sigma^{*0}$, and small for the $\gamma^*\Sigma^- \rightarrow \Sigma^{*-}$ and $\gamma^*\Xi^- \rightarrow \Xi^{*-}$ transitions. These results can be explained as a consequence of U -spin symmetry [22].

In order to get an idea about the order of the violation of U -spin symmetry, we consider the ratio $\left| (G_M^{\Sigma^+} / G_M^{\Xi^0}) - 1 \right|$. In the case of U -spin symmetry this quantity should be equal to zero. Our numerical results show that this quantity is about 0.3, i.e., the violation of U -spin symmetry is about 30%. On the other hand, in the case of the $\gamma^*\Sigma^- \rightarrow \Sigma^{*-}$ and $\gamma^*\Xi^- \rightarrow \Xi^{*-}$ transitions, the above-considered ratio is approximately equal to 2.0, which is an identification of the highly broken U -spin symmetry. It should be remembered here

that, the values of $G_M(Q^2)$ for these transitions are quite small and they are very sensitive to the values of the input parameters.

For completeness, we can also compare our results with the quark model predictions by means of the ratios $R_1 = (G_M^{\Sigma^+})_{quark}/(G_M^{\Sigma^+})_{our}$ and $R_2 = (G_M^{\Xi^0})_{quark}/(G_M^{\Xi^0})_{our}$. Our analysis shows that these ratios vary in the range 1.3 to 1.4 in accordance with their dependence on Q^2 . In other words, the difference among our predictions and those of the quark model results is about 40%.

The U -spin symmetry allows us to obtain the relations among the form factors of $\gamma^*\Lambda \rightarrow \Sigma^{*0}$ and $\gamma^*N \rightarrow \Delta$ transitions, the latter of which has already been measured in the experiments. One can easily find that the form factors in the aforementioned transitions differ from each other by a factor of $\sqrt{3/4}$. Using this result we can compare our predictions on the multipole form factors with the predictions of [13], in which the magnetic dipole $G_M(Q^2)$ for the $\gamma^*N \rightarrow \Delta$ transition is calculated within the framework of the light cone QCD sum rules. From a comparison of our result on $G_M(Q^2)$ with the result given in [13], we see that the prediction of both works are very close to each other.

The results for the electric quadrupole $G_E(Q^2)$ and Coulomb quadrupole $G_C(Q^2)$ form factors can be summarized as follows. From our numerical results we observe that, for the $\gamma^*\Xi^0 \rightarrow \Xi^{*0}$ transition only, the electric quadrupole $G_E(Q^2)$ form factor changes its sign around $Q^2 \simeq 2.5 \text{ GeV}^2$. In the transitions $\gamma^*\Sigma^+ \rightarrow \Sigma^{*+}$, $\gamma^*\Sigma^0 \rightarrow \Sigma^{*0}$, $\gamma^*\Lambda \rightarrow \Sigma^{*0}$, $\gamma^*\Xi^- \rightarrow \Xi^{*-}$ and $\gamma^*\Sigma^- \rightarrow \Sigma^{*-}$, the values of the electric quadrupole $G_E(Q^2)$ form factors are negative in the range $0.0 \leq Q^2 \leq 8.0 \text{ GeV}^2$. Note that the maximum value of the electric quadrupole $G_E(Q^2)$ is about 0.06.

The behavior of the Coulomb quadrupole $G_C(Q^2)$ form factor for the $\gamma^*\Sigma^+ \rightarrow \Sigma^{*+}$ and $\gamma^*\Xi^0 \rightarrow \Xi^{*0}$ transitions is quite similar and the magnitude of $G_C(Q^2)$ and their values are close to each other. The maximum values of the Coulomb quadrupole $G_C(Q^2)$ form factor for the $\gamma^*\Sigma^0 \rightarrow \Sigma^{*0}$ and $\gamma^*\Lambda \rightarrow \Sigma^{*0}$ transitions are very close to each other. they are about 0.10–0.15. For the $\gamma^*\Sigma^- \rightarrow \Sigma^{*-}$ and $\gamma^*\Xi^- \rightarrow \Xi^{*-}$ transitions, the values of $G_C(Q^2)$ are small. Their maximum value is about 0.012.

A comparison of our results on magnetic dipole form factor $G_M(Q^2)$ with those given in [11] would be quite useful. Our predictions on the magnitude of $G_M(Q^2)$ for the $\gamma^*\Xi^0 \rightarrow \Xi^{*0}$, $\gamma^*\Lambda \rightarrow \Sigma^{*0}$, $\gamma^*\Sigma^0 \rightarrow \Sigma^{*0}$, and $\gamma^*\Sigma^+ \rightarrow \Sigma^{*+}$ transitions are smaller compared to the ones obtained from the quark model, while it is contrary to this case for the $\gamma^*\Xi^- \rightarrow \Xi^{*-}$ transition.

We finally study the Q^2 dependence of the ratios R_{EM} and R_{SM} [see Eq. (4)].

In Figs (9) and (10) we study the Q^2 dependence of the ratios R_{EM} and R_{SM} on Q^2 , respectively. We see from Fig. (9) that the predictions for R_{EM} for the $\gamma^*\Sigma^- \rightarrow \Sigma^{*-}$ and $\gamma^*\Xi^- \rightarrow \Xi^{*-}$ transitions are close to each other and the values of R_{EM} for these transitions range in the regions 0.4–0.5 and 0.50–0.65, respectively. For all other transitions the maximum value R_{EM} is about 0.2. It should also be noted that the values of R_{EM} for the $\gamma^*\Sigma^+ \rightarrow \Sigma^{*+}$ and $\gamma^*\Sigma^0 \rightarrow \Sigma^{*0}$ transitions do not change considerably, while for the $\gamma^*\Xi^0 \rightarrow \Xi^{*0}$ and $\gamma^*\Lambda \rightarrow \Sigma^{*0}$ transitions R_{EM} varies from 0.0 at $Q^2 = 1.0 \text{ GeV}^2$ to 0.2 at $Q^2 = 8.0 \text{ GeV}^2$.

As far as R_{SM} is considered, our results can be summarized as follows.

- The result of R_{SM} for the case of the $\gamma^*\Sigma^- \rightarrow \Sigma^{*-}$ transition shows that R_{SM} is

practically very small when Q^2 varies in the domain $1.0 \leq Q^2 \leq 8.0 \text{ GeV}^2$.

- Similar to the previous case, the value of R_{SM} is also very small for the $\gamma^*\Xi^- \rightarrow \Xi^{*-}$ transition, which can be attributed to the U -spin symmetry. The small difference in the results has its roots in the violation of $SU(3)$ symmetry.
- The values of R_{SM} for the $\gamma^*\Lambda \rightarrow \Sigma^{*0}$ transition run in the range 0.2–0.3.
- Furthermore, the behavior of R_{SM} for the $\gamma^*\Sigma^+ \rightarrow \Sigma^{*+}$ and $\gamma^*\Xi^0 \rightarrow \Xi^{*0}$ transitions seems to be practically independent of Q^2 , and is about 0.25 and 0.35, respectively.
- As we consider the $\gamma^*\Sigma^0 \rightarrow \Sigma^{*0}$ transition, we observe that it exhibits sensitivity to the variation of Q^2 , and R_{SM} changes in the range 0.35–0.50.

Determination of the multipole form factors for the γ^* *octet* \rightarrow *decuplet* transitions from future experiments would be quite valuable in checking the predictions of various theoretical models and for choosing the “right” model of hadrons. In this sense our predictions might shed light on a deeper understanding of the inner structure of hadrons.

The results presented in this work can be improved by extending the calculations for the DAs to the next-to-leading order of the conformal spin and by taking $\mathcal{O}(\alpha_s)$ corrections into account.

In conclusion, in this work we study the multipole form factors, namely, magnetic dipole $G_M(Q^2)$, electric quadrupole $G_E(Q^2)$, and Coulomb quadrupole $G_C(Q^2)$ form factors, describing the octet to decuplet electromagnetic transitions within the light cone QCD sum rules. We compare our results on the magnetic dipole $G_M(Q^2)$ form factor with the predictions of the spectator quark model [11] and see that our results are smaller in magnitude than those predicted in [11], except for the $\gamma^*\Xi^- \rightarrow \Xi^{*-}$ transition. We next study the Q^2 dependence of the ratios of electric quadrupole $G_E(Q^2)$ and Coulomb quadrupole $G_C(Q^2)$ form factors to the magnetic dipole $G_M(Q^2)$ form factor.

Appendix A

For completeness, in this appendix we present the general Lorentz decomposition of the matrix element of the three-quark operators between the vacuum and the octet baryon states in terms of the DAs [15].

$$\begin{aligned}
4 \langle 0 | \varepsilon^{ijk} u_\alpha^i(a_1 x) u_\beta^j(a_2 x) d_\gamma^k(a_3 x) | \mathcal{O}(p) \rangle = & \\
& \mathcal{S}_1 m_\mathcal{O} C_{\alpha\beta} (\gamma_5 \mathcal{O})_\gamma + \mathcal{S}_2 m_\mathcal{O}^2 C_{\alpha\beta} (\not{x} \gamma_5 \mathcal{O})_\gamma + \mathcal{P}_1 m_\mathcal{O} (\gamma_5 C)_{\alpha\beta} \mathcal{O}_\gamma + \mathcal{P}_2 m_\mathcal{O}^2 (\gamma_5 C)_{\alpha\beta} (\not{x} \mathcal{O})_\gamma \\
& + \left(\mathcal{V}_1 + \frac{x^2 m_\mathcal{O}^2}{4} \mathcal{V}_1^M \right) (\not{p} C)_{\alpha\beta} (\gamma_5 \mathcal{O})_\gamma + \mathcal{V}_2 m_\mathcal{O} (\not{p} C)_{\alpha\beta} (\not{x} \gamma_5 \mathcal{O})_\gamma + \mathcal{V}_3 m_\mathcal{O} (\gamma_\mu C)_{\alpha\beta} (\gamma^\mu \gamma_5 \mathcal{O})_\gamma \\
& + \mathcal{V}_4 m_\mathcal{O}^2 (\not{x} C)_{\alpha\beta} (\gamma_5 \mathcal{O})_\gamma + \mathcal{V}_5 m_\mathcal{O}^2 (\gamma_\mu C)_{\alpha\beta} (i \sigma^{\mu\nu} x_\nu \gamma_5 \mathcal{O})_\gamma + \mathcal{V}_6 m_\mathcal{O}^3 (\not{x} C)_{\alpha\beta} (\not{x} \gamma_5 \mathcal{O})_\gamma \\
& + \left(\mathcal{A}_1 + \frac{x^2 m_\mathcal{O}^2}{4} \mathcal{A}_1^M \right) (\not{p} \gamma_5 C)_{\alpha\beta} \mathcal{O}_\gamma + \mathcal{A}_2 m_\mathcal{O} (\not{p} \gamma_5 C)_{\alpha\beta} (\not{x} \mathcal{O})_\gamma + \mathcal{A}_3 m_\mathcal{O} (\gamma_\mu \gamma_5 C)_{\alpha\beta} (\gamma^\mu \mathcal{O})_\gamma \\
& + \mathcal{A}_4 m_\mathcal{O}^2 (\not{x} \gamma_5 C)_{\alpha\beta} \mathcal{O}_\gamma + \mathcal{A}_5 m_\mathcal{O}^2 (\gamma_\mu \gamma_5 C)_{\alpha\beta} (i \sigma^{\mu\nu} x_\nu \mathcal{O})_\gamma + \mathcal{A}_6 m_\mathcal{O}^3 (\not{x} \gamma_5 C)_{\alpha\beta} (\not{x} \mathcal{O})_\gamma \\
& + \left(\mathcal{T}_1 + \frac{x^2 m_\mathcal{O}^2}{4} \mathcal{T}_1^M \right) (p^\nu i \sigma_{\mu\nu} C)_{\alpha\beta} (\gamma^\mu \gamma_5 \mathcal{O})_\gamma + \mathcal{T}_2 m_\mathcal{O} (x^\mu p^\nu i \sigma_{\mu\nu} C)_{\alpha\beta} (\gamma_5 \mathcal{O})_\gamma \\
& + \mathcal{T}_3 m_\mathcal{O} (\sigma_{\mu\nu} C)_{\alpha\beta} (\sigma^{\mu\nu} \gamma_5 \mathcal{O})_\gamma + \mathcal{T}_4 m_\mathcal{O} (p^\nu \sigma_{\mu\nu} C)_{\alpha\beta} (\sigma^{\mu\rho} x_\rho \gamma_5 \mathcal{O})_\gamma \\
& + \mathcal{T}_5 m_\mathcal{O}^2 (x^\nu i \sigma_{\mu\nu} C)_{\alpha\beta} (\gamma^\mu \gamma_5 \mathcal{O})_\gamma + \mathcal{T}_6 m_\mathcal{O}^2 (x^\mu p^\nu i \sigma_{\mu\nu} C)_{\alpha\beta} (\not{x} \gamma_5 \mathcal{O})_\gamma \\
& + \mathcal{T}_7 m_\mathcal{O}^2 (\sigma_{\mu\nu} C)_{\alpha\beta} (\sigma^{\mu\nu} \not{x} \gamma_5 \mathcal{O})_\gamma + \mathcal{T}_8 m_\mathcal{O}^3 (x^\nu \sigma_{\mu\nu} C)_{\alpha\beta} (\sigma^{\mu\rho} x_\rho \gamma_5 \mathcal{O})_\gamma ,
\end{aligned}$$

where C is the charge conjugation operator, and \mathcal{O} represents the octet baryon with momentum p .

Appendix B

In this appendix we present the expressions for the functions ρ_2 , ρ_4 and ρ_6 which appear in the sum rules for $G_1(Q^2)$, $G_2(Q^2)$, and $\frac{G_2(Q^2)}{2} - G_3(Q^2)$, for the $\gamma^*\Sigma^+ \rightarrow \Sigma^{*+}$ and $\gamma^*\Sigma^0 \rightarrow \Sigma^{*0}$ transitions.

$\gamma^*\Sigma^+ \rightarrow \Sigma^{*+}$ transition

$$\begin{aligned}
 (\rho_4)_1^{\Sigma^{*+}}(x) &= 4e_{q_3}m_{\mathcal{O}}^2\widehat{\widehat{B}}_6(x) - 8e_{q_2}m_{\mathcal{O}}m_{q_2}\widetilde{B}_2(x) - 8e_{q_3}m_{\mathcal{O}}m_{q_3}\widehat{B}_4(x) \\
 &\quad - 8e_{q_2}m_{\mathcal{O}}^2\int_0^{\bar{x}} dx_1\left[A_1^M - T_1^M\right](x_1, x, 1-x_1-x) \\
 &\quad - 8e_{q_3}m_{\mathcal{O}}^2\int_0^{\bar{x}} dx_1 T_1^M(x_1, 1-x_1-x, x)
 \end{aligned}$$

$$\begin{aligned}
 (\rho_2)_1^{\Sigma^{*+}}(x) &= -8e_{q_2}\int_0^{\bar{x}} dx_1\left[A_1 - T_1\right](x_1, x, 1-x_1-x) \\
 &\quad - 8e_{q_3}\int_0^{\bar{x}} dx_1 T_1(x_1, 1-x_1-x, x)
 \end{aligned}$$

$$\begin{aligned}
 (\rho_6)_2^{\Sigma^{*+}}(x) &= -64e_{q_1}m_{\mathcal{O}}^3(1-x)x^2\check{C}_6(x) \\
 &\quad + 16e_{q_2}m_{\mathcal{O}}^2x\left[4m_{\mathcal{O}}(1-x)x(2\widetilde{\widetilde{B}}_8 - \widetilde{\widetilde{C}}_6) - m_{q_2}\widetilde{\widetilde{B}}_6\right](x) \\
 &\quad + 16e_{q_3}m_{\mathcal{O}}^2x\left[2m_{\mathcal{O}}(1-x)x(2\widehat{\widehat{B}}_8 - 2\widehat{\widehat{C}}_6 + \widehat{\widehat{D}}_6) + m_{q_3}\widehat{\widehat{B}}_6\right](x)
 \end{aligned}$$

$$\begin{aligned}
 (\rho_4)_2^{\Sigma^{*+}}(x) &= -8e_{q_1}m_{\mathcal{O}}(1-2x)x\check{C}_2 \\
 &\quad - 8e_{q_2}m_{\mathcal{O}}x\left[2\widetilde{B}_2 - (1-2x)(2\widetilde{B}_4 - \widetilde{C}_2) + \widetilde{D}_2\right](x) \\
 &\quad + 8e_{q_3}m_{\mathcal{O}}x\left[2(1-x)\widehat{B}_4 + x(2\widehat{C}_2 - \widehat{D}_2)\right](x)
 \end{aligned}$$

$$\begin{aligned}
 (\rho_6)_3^{\Sigma^{*+}}(x) &= 64e_{q_1}m_{\mathcal{O}}^3(1-x)^2x\check{C}_6(x) \\
 &\quad - 64e_{q_2}m_{\mathcal{O}}^3(1-x)^2x\left[2\widetilde{\widetilde{B}}_8 - \widetilde{\widetilde{C}}_6\right](x) \\
 &\quad - 32e_{q_3}m_{\mathcal{O}}^3(1-x)^2x\left[2\widehat{\widehat{B}}_8 - 2\widehat{\widehat{C}}_6 + \widehat{\widehat{D}}_6\right](x)
 \end{aligned}$$

$$\begin{aligned}
 (\rho_4)_3^{\Sigma^{*+}}(x) &= -16e_{q_1}m_{\mathcal{O}}(1-x)x\check{C}_2(x) \\
 &\quad + 16e_{q_2}m_{\mathcal{O}}(1-x)\left[\widetilde{B}_2 + x(2\widetilde{B}_4 - \widetilde{C}_2)\right](x) \\
 &\quad + 8e_{q_3}m_{\mathcal{O}}(1-x)\left[\widehat{B}_2 - (1-2x)\widehat{B}_4 + x(2\widehat{C}_2 - \widehat{D}_2)\right](x),
 \end{aligned}$$

where $q_1 = q_2 = u$, $q_3 = s$.

The expressions for the functions ρ_2 , ρ_4 and ρ_6 describing the $\gamma^*\Xi^0 \rightarrow \Xi^{*0}$ and $\gamma^*\Xi^- \rightarrow \Xi^{*-}$ transitions can be obtained from the corresponding results of the $\gamma^*\Sigma^+ \rightarrow \Sigma^{*+}$ transition by making the replacements $u \leftrightarrow s$ (for the $\gamma^*\Xi^0 \rightarrow \Xi^{*0}$), and $u \rightarrow s$, $s \rightarrow d$ (for the $\gamma^*\Xi^- \rightarrow \Xi^{*-}$).

$\gamma^*\Sigma^0 \rightarrow \Sigma^{*0}$ transition

$$\begin{aligned}
(\rho_4)_1^{\Sigma^{*0}}(x) &= 4e_{q_3}m_{\mathcal{O}}^2\widehat{B}_6(x) - 4e_{q_1}m_{q_1}m_{\mathcal{O}}\check{B}_2(x) - 4e_{q_2}m_{\mathcal{O}}m_{q_2}\widetilde{B}_2(x) - 8e_{q_3}m_{\mathcal{O}}m_{q_3}\widehat{B}_4(x) \\
&\quad + 4e_{q_1}m_{\mathcal{O}}^2\int_0^{\bar{x}} dx_3 [A_1^M + T_1^M](x, 1-x-x_3, x_3) \\
&\quad - 4e_{q_2}m_{\mathcal{O}}^2\int_0^{\bar{x}} dx_1 [A_1^M - T_1^M](x_1, x, 1-x_1-x) \\
&\quad - 8e_{q_3}m_{\mathcal{O}}^2\int_0^{\bar{x}} dx_1 T_1^M(x_1, 1-x_1-x, x)
\end{aligned}$$

$$\begin{aligned}
(\rho_2)_1^{\Sigma^{*0}}(x) &= 4e_{q_1}\int_0^{\bar{x}} dx_3 [A_1 + T_1](x, 1-x-x_3, x_3) \\
&\quad - 4e_{q_2}\int_0^{\bar{x}} dx_1 [A_1 - T_1](x_1, x, 1-x_1-x) \\
&\quad - 8e_{q_3}\int_0^{\bar{x}} dx_1 T_1(x_1, 1-x_1-x, x)
\end{aligned}$$

$$\begin{aligned}
(\rho_6)_2^{\Sigma^{*0}}(x) &= 16e_{q_1}m_{\mathcal{O}}^2x[4m_{\mathcal{O}}(1-x)x(\check{B}_8 - \check{C}_6) - m_{q_1}\check{B}_6](x) \\
&\quad + 64e_{q_2}m_{\mathcal{O}}^3(1-x)x^2[\widetilde{B}_8 - \widetilde{C}_6](x) \\
&\quad + 16e_{q_3}m_{\mathcal{O}}^2x[4m_{\mathcal{O}}(1-x)x(\widehat{B}_8 - \widehat{C}_6) + m_{q_3}\widehat{B}_6](x)
\end{aligned}$$

$$\begin{aligned}
(\rho_4)_2^{\Sigma^{*0}}(x) &= 4e_{q_1}m_{\mathcal{O}}x[2(1-2x)(\check{B}_4 - \check{C}_2) - 2\check{B}_2 + \check{D}_2](x) \\
&\quad - 4e_{q_2}m_{\mathcal{O}}x[2\widetilde{B}_2 - 2(1-2x)(\widetilde{B}_4 - \widetilde{C}_2) + \widetilde{D}_2](x) \\
&\quad + 16e_{q_3}m_{\mathcal{O}}x[(1-x)\widehat{B}_4 + x\widehat{C}_2](x)
\end{aligned}$$

$$\begin{aligned}
(\rho_6)_3^{\Sigma^{*0}}(x) &= -64e_{q_1}m_{\mathcal{O}}^3(1-x)^2x[\check{B}_8 - \check{C}_6](x) \\
&\quad - 64e_{q_2}m_{\mathcal{O}}^3(1-x)^2x[\widetilde{B}_8 - \widetilde{C}_6](x) \\
&\quad - 64e_{q_3}m_{\mathcal{O}}^3(1-x)^2x[\widehat{B}_8 - \widehat{C}_6](x)
\end{aligned}$$

$$\begin{aligned}
(\rho_4)_3^{\Sigma^{*0}}(x) &= 8e_{q_1}m_{\mathcal{O}}(1-x)[\check{B}_2 - (1-2x)\check{B}_4 - 2x\check{C}_2](x) \\
&\quad + 8e_{q_2}m_{\mathcal{O}}(1-x)[\widetilde{B}_2 - (1-2x)\widetilde{B}_4 - 2x\widetilde{C}_2](x)
\end{aligned}$$

$$+ 8e_{q_3} m_{\mathcal{O}}(1-x) \left[\widehat{B}_2 - (1-2x)\widehat{B}_4 - 2x\widehat{C}_2 \right](x) ,$$

where $q_1 = u$, $q_2 = d$, and $q_3 = s$, respectively.

In the above expressions for ρ_i and ρ'_i , the functions $\mathcal{F}(x_i)$ are defined in the following way:

$$\begin{aligned} \check{\mathcal{F}}(x_1) &= \int_1^{x_1} dx'_1 \int_0^{1-x'_1} dx_3 \mathcal{F}(x'_1, 1-x'_1-x_3, x_3) , \\ \check{\check{\mathcal{F}}}(x_1) &= \int_1^{x_1} dx'_1 \int_1^{x'_1} dx''_1 \int_0^{1-x''_1} dx_3 \mathcal{F}(x''_1, 1-x''_1-x_3, x_3) , \\ \widetilde{\mathcal{F}}(x_2) &= \int_1^{x_2} dx'_2 \int_0^{1-x'_2} dx_1 \mathcal{F}(x_1, x'_2, 1-x_1-x'_2) , \\ \widetilde{\widetilde{\mathcal{F}}}(x_2) &= \int_1^{x_2} dx'_2 \int_1^{x'_2} dx''_2 \int_0^{1-x''_2} dx_1 \mathcal{F}(x_1, x''_2, 1-x_1-x''_2) , \\ \widehat{\mathcal{F}}(x_3) &= \int_1^{x_3} dx'_3 \int_0^{1-x'_3} dx_1 \mathcal{F}(x_1, 1-x_1-x'_3, x'_3) , \\ \widehat{\widehat{\mathcal{F}}}(x_3) &= \int_1^{x_3} dx'_3 \int_1^{x'_3} dx''_3 \int_0^{1-x''_3} dx_1 \mathcal{F}(x_1, 1-x_1-x''_3, x''_3) . \end{aligned}$$

Definitions of the functions B_i , C_i , D_i , E_1 and H_1 that appear in the expressions for $\rho_i(x)$ are given as follows:

$$\begin{aligned} B_2 &= T_1 + T_2 - 2T_3 , \\ B_4 &= T_1 - T_2 - 2T_7 , \\ B_5 &= -T_1 + T_5 + 2T_8 , \\ B_6 &= 2T_1 - 2T_3 - 2T_4 + 2T_5 + 2T_7 + 2T_8 , \\ B_7 &= T_7 - T_8 , \\ B_8 &= -T_1 + T_2 + T_5 - T_6 + 2T_7 + 2T_8 , \\ C_2 &= V_1 - V_2 - V_3 , \\ C_4 &= -2V_1 + V_3 + V_4 + 2V_5 , \\ C_5 &= V_4 - V_3 , \\ C_6 &= -V_1 + V_2 + V_3 + V_4 + V_5 - V_6 , \\ D_2 &= -A_1 + A_2 - A_3 , \\ D_4 &= -2A_1 - A_3 - A_4 + 2A_5 , \\ D_5 &= A_3 - A_4 , \\ D_6 &= A_1 - A_2 + A_3 + A_4 - A_5 + A_6 , \\ E_1 &= S_1 - S_2 , \\ H_1 &= P_2 - P_1 . \end{aligned}$$

References

- [1] I. G. Aznauryan, A. Bashir, V. Braun, S. J. Brodsky *et. al*, Int. J. Mod. Phys. E **22**, 1330015 (2013).
- [2] S. Taylor *et. al* (CLAS Collaboration), Phys. Rev. C **71**, 054630 (2005).
- [3] V. Molchanov *et. al*, Phys. Lett. B **590**, 161 (2004).
- [4] R. Koniuk and N. Isgur, Phys. Rev. D **21**, 1868 (1980); Phys. Rev. D **23**, 818(E) (1981).
- [5] G. Wagner, A. J. Buchmann and A. Faessler, Phys. Rev. C **58**, 1745 (1998).
- [6] N. Sharma, H. Dahiya, P. K. Chatley, and M. Gupta, Phys. Rev. D **81**, 073001 (2010).
- [7] N. Sharma, and H. Dahiya, Pramana J. Phys. **80**, 237 (2013); Pramana J. Phys. **80**, 1083(E#) (2013).
- [8] L. Wang, and F. X. Lee, Phys. Rev. D **80**, 0340031 (2009).
- [9] T. M. Aliev and A. Özpineci, Nucl.Phys. B **732**, 291 (2006).
- [10] D. B. Leinweber, T. Drapa, and R. M. Woloshyn, Phys. Rev. D **48**, 2230 (1993).
- [11] G. Ramalho and K. Tsushima, Phys. Rev. D **87**, 093011 (2013).
- [12] C. Alexandrou, G. Kountson, H. Neff, J. W. Negele, W. Schroers, and A. Tsapalis, Phys. Rev. D **77**, 085012 (2008).
- [13] V. M. Braun, A. Lenz, G. Peters, and A. V. Radyushkin, Phys. Rev. D **73**, 034020 (2006).
- [14] H. F. Jones, and M. D. Scadron, Ann. Phys. (N.Y.) **81**, 1 (1973).
- [15] V. M. Braun, R. J. Fries, N. Mahnke, and E. Stein, Nucl.Phys. B **589**, 381 (2000); Nucl.Phys. B **607**, 433 (2001).
- [16] A. Lenz, M. Gockeler, T. Kaltenbrunner, and N. Warkentin, Phys. Rev. D **79**, 039007 (2009).
- [17] Y.-L. Liu, M.-Q. Huang, Nucl.Phys. A **8210**, 80 (2009).
- [18] Y.-L. Liu, M.-Q. Huang, Phys. Rev. D **80**, 055015 (2009).
- [19] Y.-L. Liu, M.-Q. Huang, J. Phys. G **37**, 115010 (2010).
- [20] Y.-L. Liu, M.-Q. Huang, Phys. Rev. D **79**, 114031 (2009).
- [21] V. M. Belyaev and B. L. Ioffe, Sov. Phys. JETP **57**, 716 (1983).
- [22] H. J. Lipkin, Phys. Rev. D **7**, 846 (1973).

Figure captions

Fig. (1) The dependence of the magnetic dipole form factor $G_M(Q^2)$ of the $\gamma^*\Sigma^+ \rightarrow \Sigma^{*+}$ transition on Q^2 at $s_0 = 4.0 \text{ GeV}^2$ and at several different fixed values of the Borel mass parameter M^2 .

Fig. (2) The same as in Fig. (1), but for the electric quadrupole $G_E(Q^2)$ form factor.

Fig. (3) The same as in Fig. (1), but for the Coulomb quadrupole $G_C(Q^2)$ form factor.

Fig. (4) The same as in Fig. (1), but for the $\gamma^*\Lambda \rightarrow \Sigma^{*0}$ transition.

Fig. (5) The same as in Fig. (1), but for the $\gamma^*\Sigma^0 \rightarrow \Sigma^{*0}$ transition.

Fig. (6) The same as in Fig. (1), but for the $\gamma^*\Sigma^- \rightarrow \Sigma^{*-}$ transition.

Fig. (7) The same as in Fig. (1), but for the $\gamma^*\Xi^- \rightarrow \Xi^{*-}$ transition.

Fig. (8) The same as in Fig. (1), but for the $\gamma^*\Xi^0 \rightarrow \Xi^{*0}$ transition.

Fig. (9) The dependence of the the ratio R_{EM} on Q^2 for the octet to decuplet electromagnetic transitions, at $s_0 = 4.0 \text{ GeV}^2$ and $M^2 = 2 \text{ GeV}^2$.

Fig. (10) The same as in Fig. (9), but for the ratio R_{SM} .

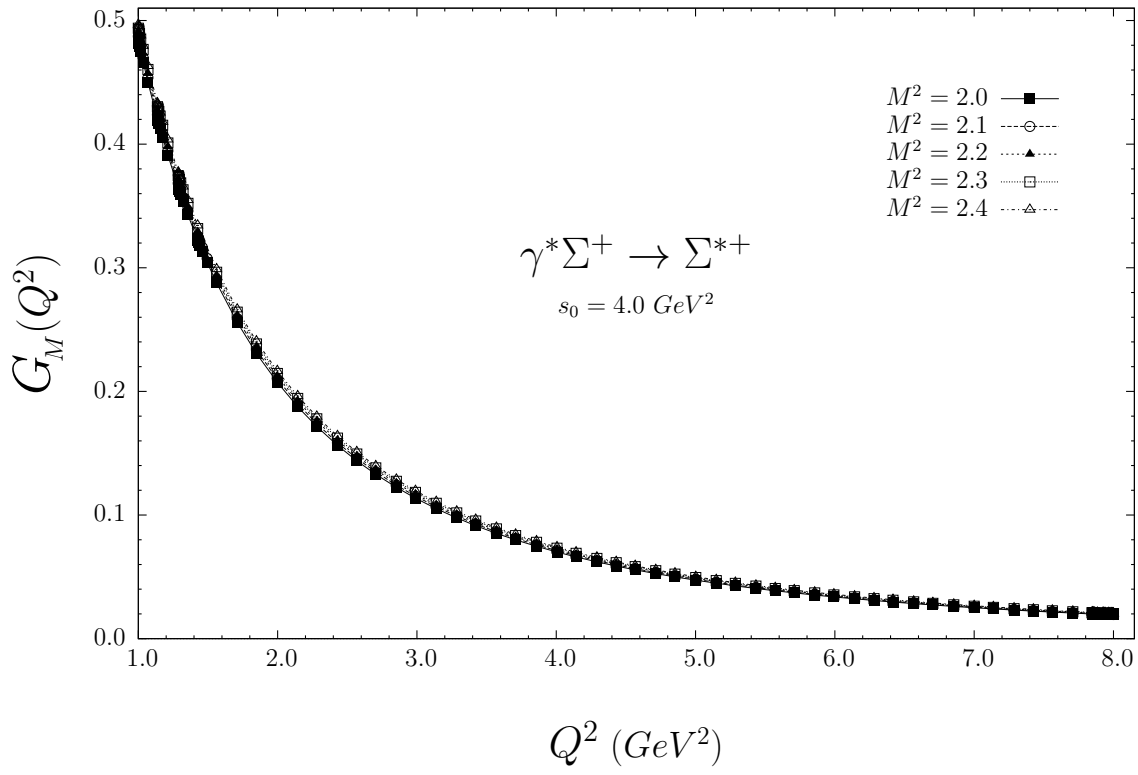


Figure 1:

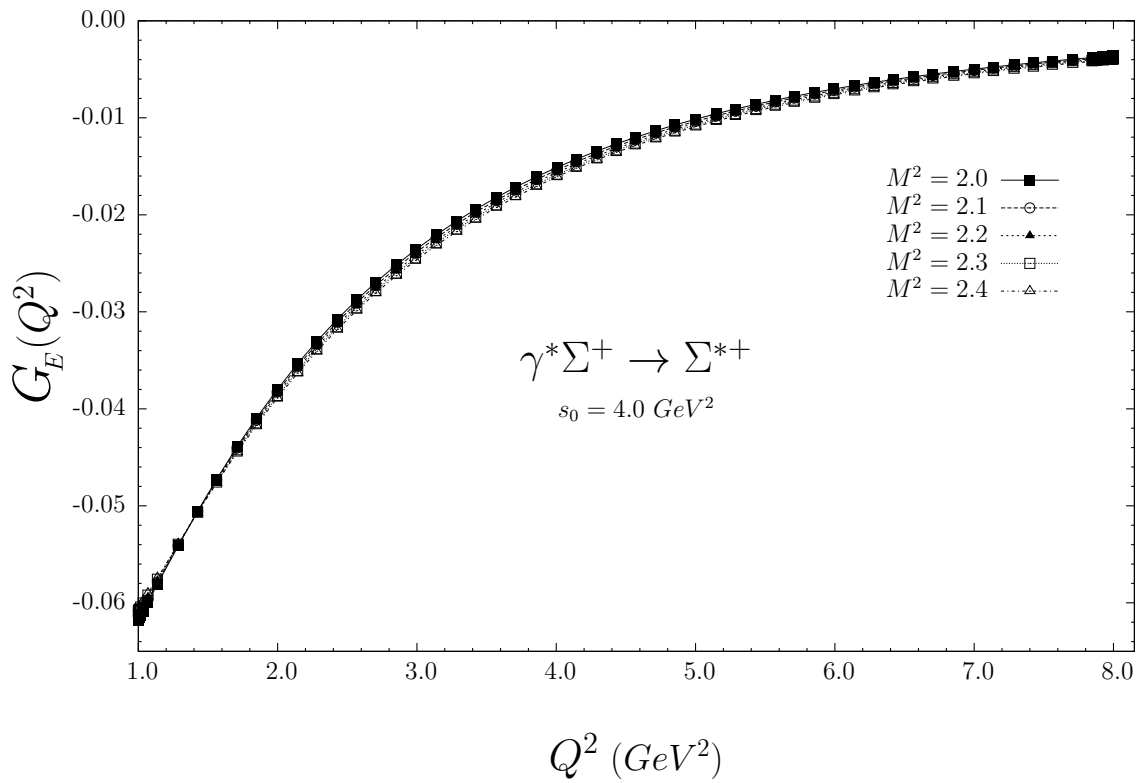


Figure 2:

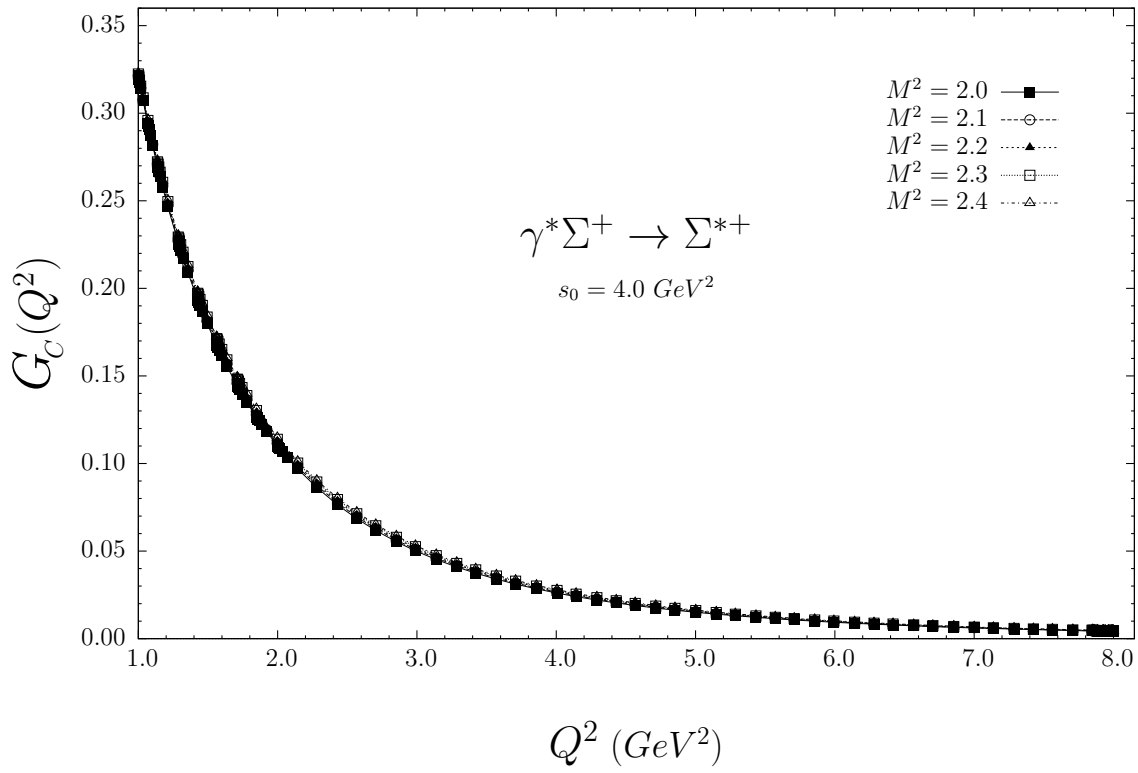


Figure 3:

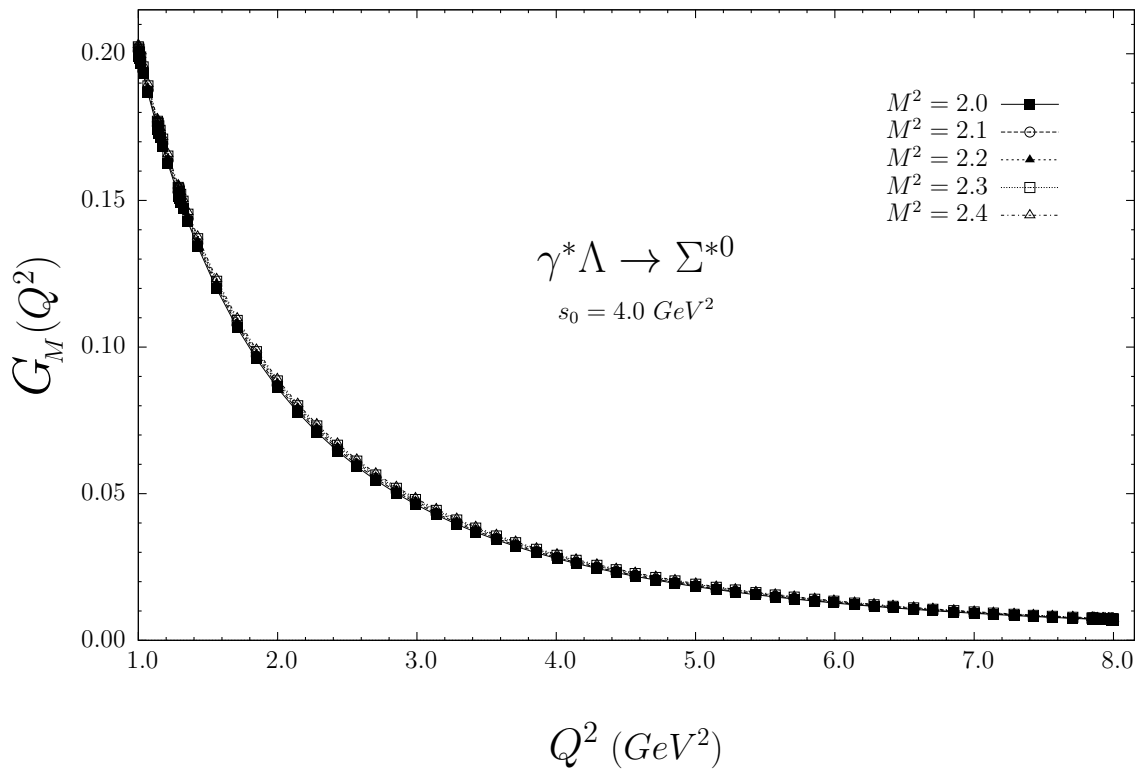


Figure 4:

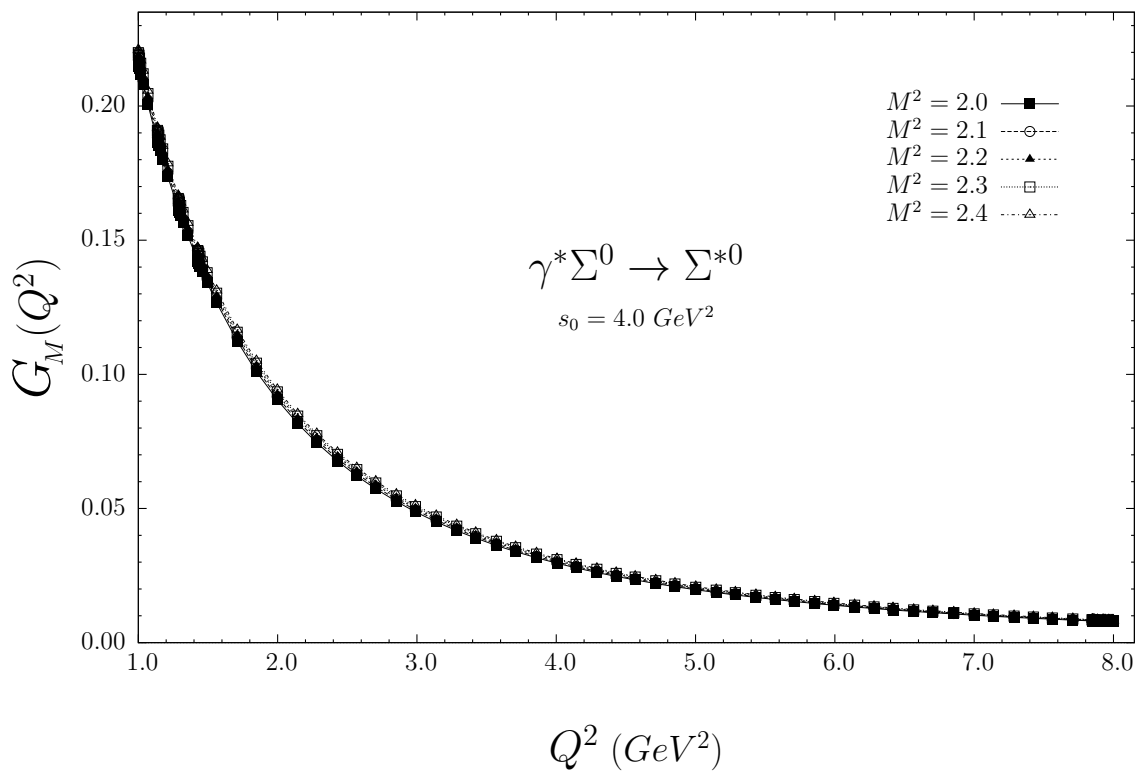


Figure 5:

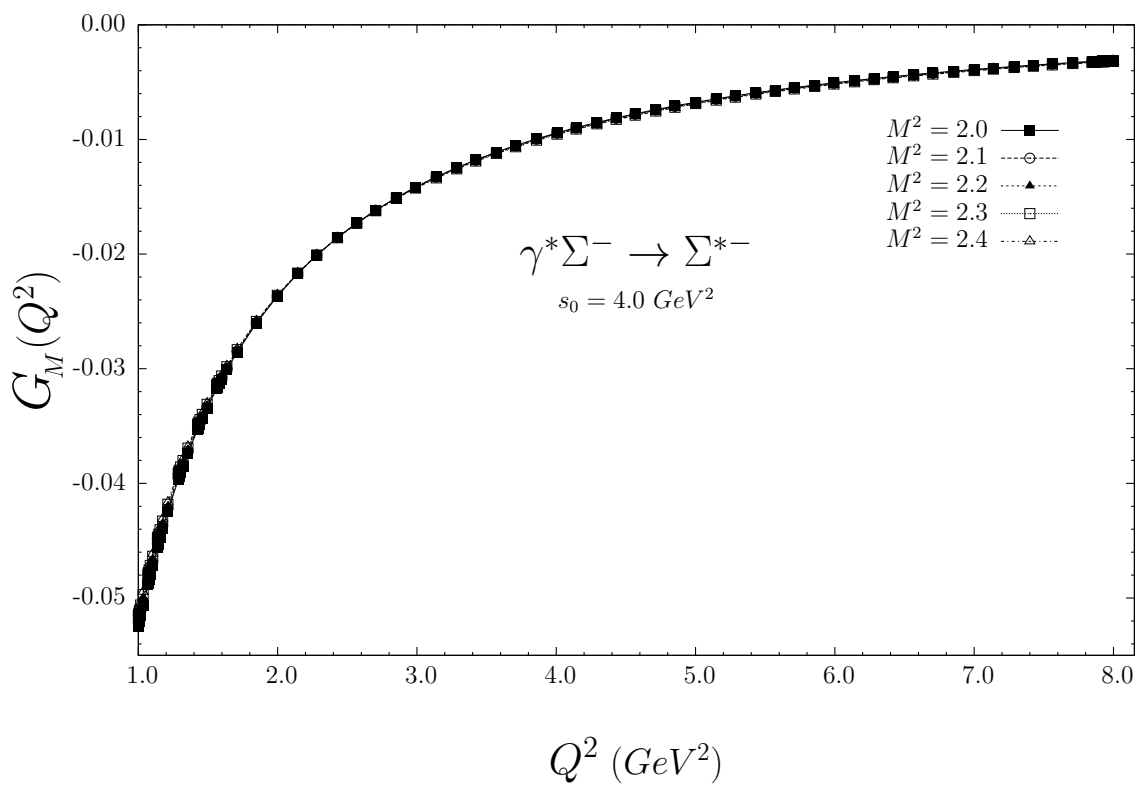


Figure 6:

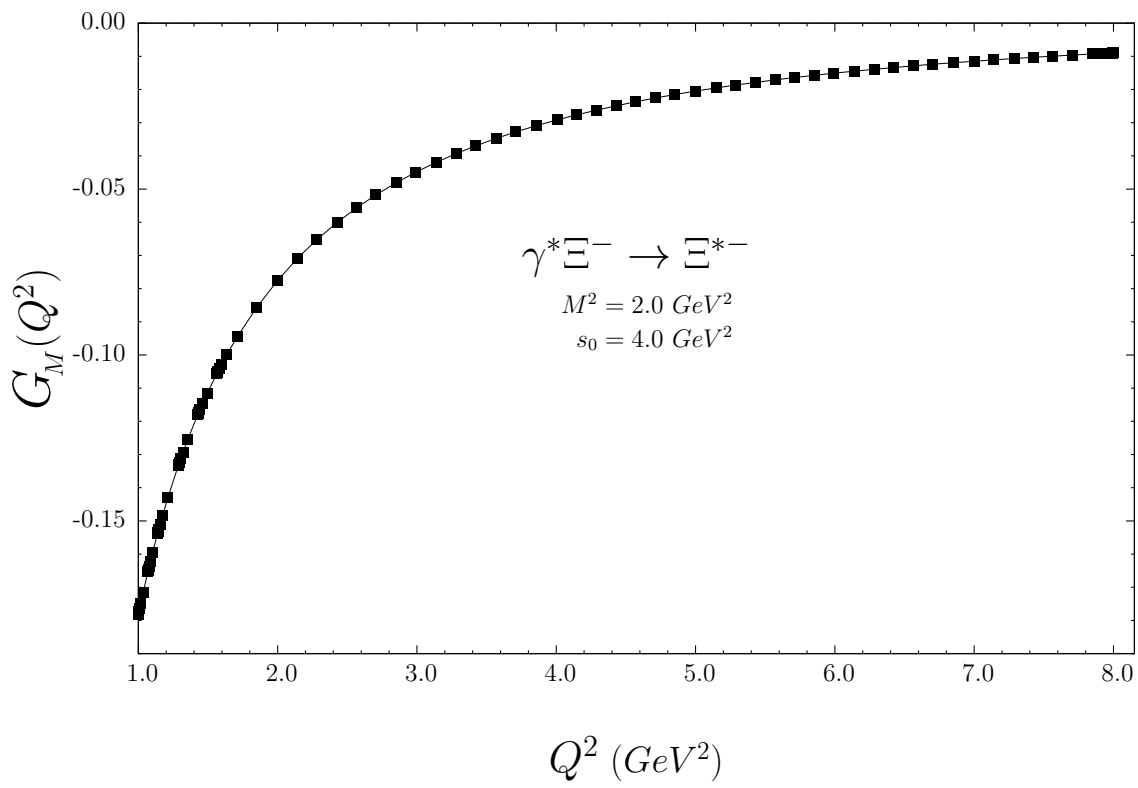


Figure 7:

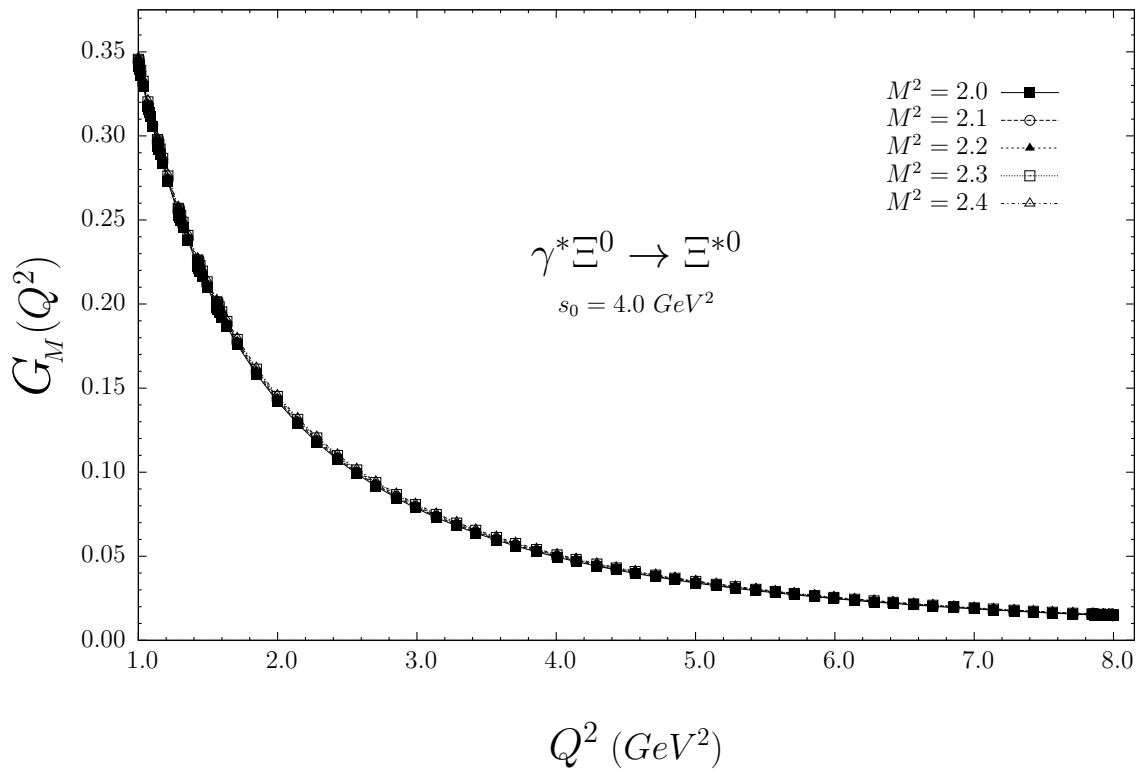


Figure 8:

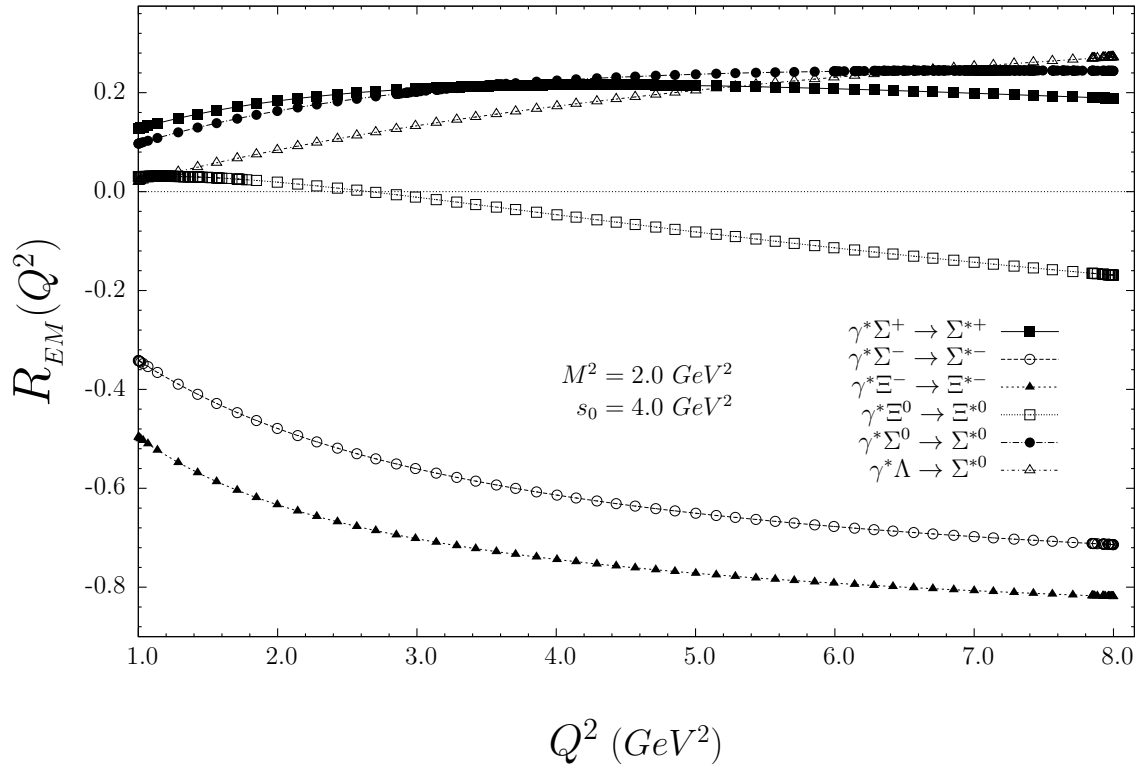


Figure 9:

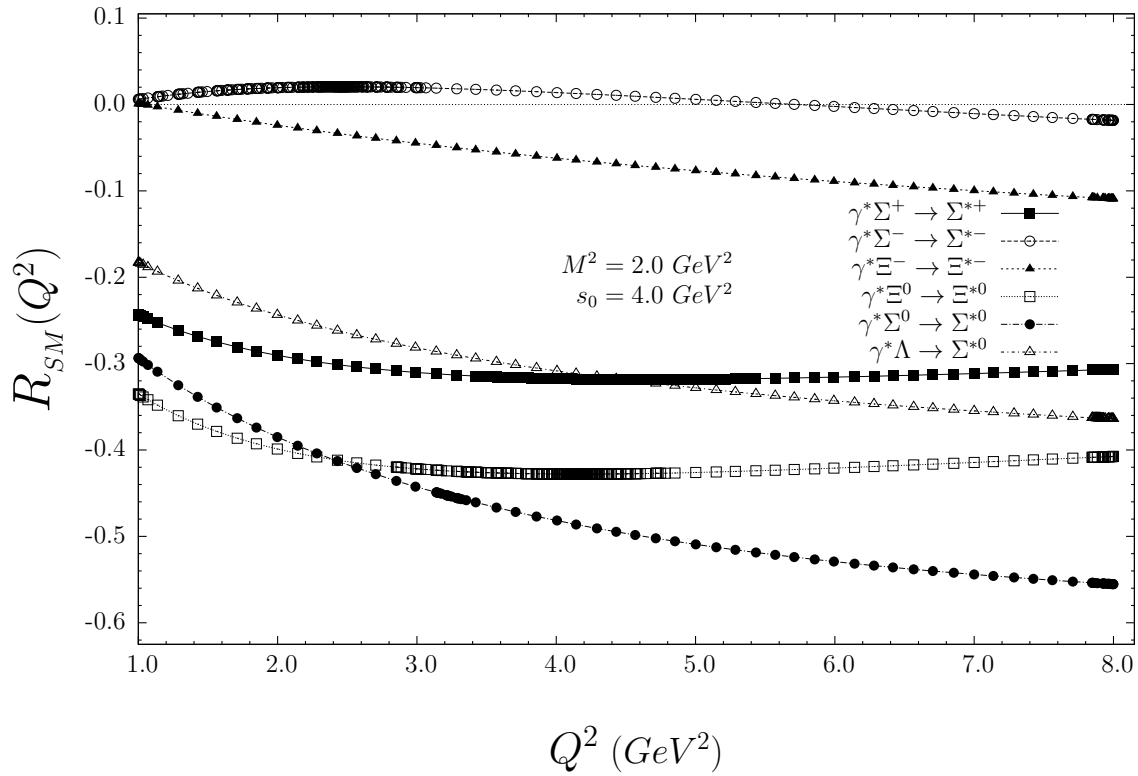


Figure 10: